Effects of Superstrate Layer on the Resonant Characteristics of Annular- Ring printed Antenna

Fadila Benmeddour, Christophe Dumond, Elhadi Kenane

The Eurasia Proceedings of Science, Technology, Engineering & Mathematics (EPSTEM)
ISSN: 2602-3199

The Eurasia Proceedings of Science, Technology, Engineering & Mathematics (EPSTEM), 2019

Volume 7, Pages 147-154

IConTES 2019: International Conference on Technology, Engineering and Science

Effects of Superstrate Layer on the Resonant Characteristics of Annular-Ring printed Antenna

Fadila BENMEDDOUR
University of M'Sila

Christophe DUMOND
Université d'Orléans

Elhadi KENANE
University of M'Sila

Abstract: In practice, it was found that the choice of the substrate or superstrate material of printed antennas is of a great importance and plays a significant role in achieving the optimum resonant characteristics of the antenna; Uniaxial dielectrics have drawn more attention due to their availability in materials such as sapphire, boron nitride and Epsilam-10 ceramic-impregnated Tefon. Previous studies of anisotropic materials used in microwave devices indicate that the effects of anisotropy on the performance of such structures particularly in high frequencies cannot be ignored. Three very popular full wave methods that can be used to characterise microstrip patch antennas are: the finite element method, the finite difference time domain method, and the moment method. The last one also known as the full-wave method is arguably the most popular method for the analysis of microstrip antennas. In this work, resonant characteristics (the resonant frequency, the Half-power bandwidth) of an annular microstrip patch printed on uniaxially anisotropic substrate and covered with an anisotropic superstrate layer are studied using an electric field integral equation and the spectral domain Green's function. In order to validate the present method, we have confronted our results with theoretical and experimental data from the literature and very Good agreements were obtained between our computed data and measurements, and the convergence of the method is proven.

Keywords: Annular-ring patch, Anisotropic, Superstrate, Resonance frequency

Introduction

Because microstrip antennas are small, lightweight, and low-cost, they have found widespread applications in satellite and wireless mobile communication systems (Garg, Bhartia, Bahl, & Ittipiboon, 1995) (James, P. S. Hall, Hall, & Wood, 1981) (Sung & Kim, 2005) (Balanis, 1997).

In practice, it was found that the choice of the substrate or superstrate material is of a great importance and plays a significant role in achieving the optimum resonant characteristics of the antenna (Bhartia, Rao, & Tomar, 1991).

Uniaxial dielectrics have drawn more attention due to their availability in materials such as sapphire, boron nitride and Epsilam-10 ceramic-impregnated Teflon. Previous studies of anisotropic materials used in microwave devices indicate that the effects of anisotropy on the performance of such structures particularly in high frequencies cannot be ignored (Gurel & Yazgan, 2003).

Several methods exist for the analysis of annular microstrip antennas. These methods can be classified as the approximate and the full-wave methods. Some of the popular approximate models include: the transmission-line model, the cavity model and the segmentation model. These models usually consider the microstrip patch as a transmission line or as a cavity resonator (Lee, Luc, & Dahele, 1988) (Biswas & Guha, 2009).

- Selection and peer-review under responsibility of the Organizing Committee of the Conference

Although the accuracy of these approximate models is limited, they are nevertheless useful in providing the preliminary design and predicting the trends of these characteristics with the variation of the design parameters.
Three very popular full wave methods that can be used to characterise microstrip patch antennas are: the finite element method, the finite difference time domain method, and the moment method (Kumar & Ray, 2003). The last one also known as the full-wave method is arguably the most popular method for the analysis of microstrip antennas (Losada, Boix, & Horno, 1999) (Bouttout, Benabdelaziz, Benghalia, Khedrouche, & Fortaki, 1999) (BahI & Bbartia, 1980) and will be used in our work. For that, a rigorous full-wave analysis with basis modes involving is developed and applied.

Superstrate dielectric layer (or layers) or earlier known as cover layers, are often used to protect printed antennas (PA) from environmental hazards, or may be naturally formed for example: ice layers during flight or severe weather conditions (POZAR, 1983). Only after the year 1985, it was discovered that the superstrate layer many prove beneficial or detrimental to printed antenna radiation characteristics, depending on the thicknesses of the substrate and cover, as well as relative dielectric and permeability constants , it may affect adversely the antenna basic performance characteristics (POZAR, 1983) (Nicolaos, Alexopoulos, & Jackson, 1984).

For this reason, in this work the effects of superstrate Annular- Ring printed antennas using the moment method are considered in detail, so that the printed antenna performance may be understood better or a proper choice of cover parameters may be implemented to advantage in the enhancement of printed antennas.

Theory

The problem to be solved is illustrated in Figure 1. A annular-ring patch of thickness e is printed on a grounded dielectric slab of thickness h_1.
The annular ring patch dimensions are the inner radius a and the outer radius b. The substrate is characterized by the free-space permeability μ_0 and a permittivity $\varepsilon_0\varepsilon_{r1}$.
Above the radiating patch is the superstrate layer of thickness h_2 with free-space permeability μ_0 and a permittivity $\varepsilon_0\varepsilon_{r2}$.The permittivity tensor in this region is given by (Losada, Boix, & Horno, 1999) (Benmeddour, Dumond, Benabdelaziz, & Bouttout, 2011) :

$$\bar{\varepsilon} = \varepsilon_0 \begin{vmatrix} \varepsilon_x & 0 & 0 \\ 0 & \varepsilon_y & 0 \\ 0 & 0 & \varepsilon_z \end{vmatrix} \tag{1}$$

Where $\varepsilon_x = \varepsilon_y \neq \varepsilon_z$.

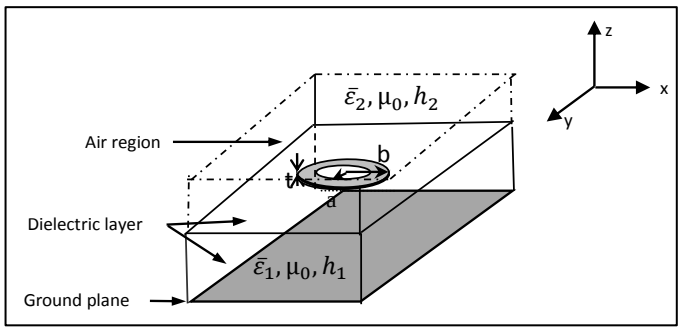

Figure 1. Geometrical structure of a superstrate loaded annular patch on a uniaxial substrate

The transverse fields components in the j[th] layer can be obtained using the vector Hankel transform formulation (Losada, Boix, & Horno, 1999) (Benmeddour, Benabdelaziz, Bouttout, & Aouabdia, 2004) (Benmeddour, Dumond, Benabdelaziz, & Bouttout, 2011).

$$E(\rho,\varphi,z) = \begin{bmatrix} E_\rho(\rho,\varphi,z) \\ E_\varphi(\rho,\varphi,z) \end{bmatrix} = \sum_{n=-\infty}^{\infty} e^{jn\varphi} \int_0^\infty dk_\rho \, k_\rho \bar{\mathbf{H}}_n(k_\rho\rho).\boldsymbol{e}_n\left(k_\rho,z\right) \tag{2}$$

$$H(\rho,\varphi,z) = \begin{bmatrix} -H_\varphi(\rho,\varphi,z) \\ E_\rho(\rho,\varphi,z) \end{bmatrix} = \sum_{n=-\infty}^{\infty} e^{jn\varphi} \int_0^\infty dk_\rho \, k_\rho \bar{\mathbf{H}}_n(k_\rho\rho).\boldsymbol{h}_n\left(k_\rho,z\right) \tag{3}$$

$\bar{\mathbf{H}}_n(k_\rho\rho)$ is the kernel of the vector Hankel transform given by (Chew & Kong, 1980).

$$\bar{\mathbf{H}}_n(k_\rho\rho)=\begin{bmatrix} j_n(k_\rho\rho) & \frac{-in}{k_\rho\rho}J_n(k_\rho\rho) \\ \frac{in}{k_\rho\rho}J_n(k_\rho\rho) & j_n(k_\rho\rho) \end{bmatrix} \tag{4}$$

$\bar{A}$ and $\bar{B}$ are two unknown vectors and is determined by :

$$\begin{aligned}\bar{\mathbf{G}}(k_\rho) &= \mathrm{diag}\left[G^{TM}, G^{TE}\right] \\ &= -\left(\bar{\mathbf{\Gamma}}_<\right)_{12}\cdot\left[\bar{\mathbf{g}}_0\cdot\left(\bar{\mathbf{\Gamma}}_>\right)_{12}-\left(\bar{\mathbf{\Gamma}}_>\right)_{22}\right]\cdot\left[\bar{\mathbf{g}}_0\cdot\left(\bar{\mathbf{\Gamma}}\right)_{12}-\left(\bar{\mathbf{\Gamma}}\right)_{22}\right]^{-1}\end{aligned} \tag{5}$$

Where

$$\bar{\Gamma}_< = \prod_{j=M}^{1}\bar{\mathrm{T}}_j\,,\ \bar{\Gamma}_> = \prod_{j=N}^{M+1}\bar{\mathrm{T}}_j\,,\ \text{and}\ \bar{\Gamma}=\bar{\Gamma}_>\cdot\bar{\Gamma}_< \tag{6}$$

$\prod_{j=M}^{1}$, and $\prod_{j=N}^{M+1}$, means the product of matrices below and above the annular ring patch.

Here, the expression of the matrices $\bar{\mathrm{T}}_j$ for the anisotropy in the dielectrics is given by :

$$\bar{\mathrm{T}}_j=\begin{bmatrix} \cos\bar{\theta}_j & i\bar{g}_j^{-1}\cdot\sin\bar{\theta}_j \\ -i\bar{g}_j\cdot\sin\bar{\theta}_j & \cos\bar{\theta}_j \end{bmatrix} \tag{7}$$

Where

$$\bar{\theta}_j=\bar{k}_{jz}d_j \tag{8}$$

In which

$$\bar{k}_{jz}=\begin{bmatrix} k_{jz}^e & 0 \\ 0 & k_{jz}^h \end{bmatrix}=\begin{bmatrix} \left(\varepsilon_{jx}k^2-\frac{\varepsilon_{jx}}{\varepsilon_{jz}}k_\rho^2\right)^{\frac{1}{2}} & 0 \\ 0 & \left(\varepsilon_{jx}k^2-k_\rho^2\right)^{\frac{1}{2}} \end{bmatrix} \tag{9}$$

$$\bar{g}_j(k_\rho)=\begin{bmatrix} \tilde{g}_j^e(k_\rho) & 0 \\ 0 & \tilde{g}_j^h(k_\rho) \end{bmatrix}=\begin{bmatrix} \frac{\omega\varepsilon_{jx}\varepsilon}{k_{jz}^h} & 0 \\ 0 & \frac{k_{jz}^e}{\omega\mu} \end{bmatrix} \tag{10}$$

and

$k=\omega\sqrt{\mu_0\varepsilon_0}$: is the free space wavenumber.

$k=\omega\sqrt{\mu\varepsilon}$: Note that the presence of an arbitrarily number of layers above and / or below the annular patch is easily included in the matrix product $\bar{\Gamma}_<$ and/ or $\bar{\Gamma}_>$.

In applying Galerkin method to solve the vector dual integral equations express the unknown annular patch current in terms of appropriate expansion modes formed expansion basis functions (Sami, Chew, & Kong, 1982).

$$\boldsymbol{\kappa}_n(\rho)=\begin{cases}\sum_{P=1}^{P}a_{np}\boldsymbol{l}_{np}(\rho)+\sum_{q=1}^{Q}b_{nq}\boldsymbol{f}_{nq}(\rho) & a<\rho<b \\ 0 & \rho>b,\rho<a\end{cases} \tag{11}$$

Here a_{np} and b_{nq} are unknown coefficients

Principal system

$$\boldsymbol{l}_{nm}(\rho)=\begin{cases}\begin{bmatrix}\psi_n'\left(\frac{\beta_{nm}\rho}{a}\right)\\ \frac{n}{\frac{\beta_{nm}\rho}{a}}\psi_n\left(\frac{\beta_{nm}\rho}{a}\right)\end{bmatrix} & a<\rho<b\\ 0 & \rho>b,\ \rho<a\end{cases} \tag{12}$$

The Hankel transform of $\boldsymbol{l}_{nm}$ is:

$$\boldsymbol{L}_{nm}(k_\rho)=\begin{bmatrix}\frac{\beta_{nm}/a}{(\beta_{nm}/a)^2-k_\rho^2}Y_{nm}'(k_\rho)\\ \frac{n}{(\beta_{nm}/a)k_\rho}Y_{nm}(k_\rho)\end{bmatrix} \tag{13}$$

Where

$$\begin{aligned}&Y_{nm}(k_\rho)=\psi_n\\ &Y_{nm}(k_\rho)=\psi_n(\beta_{nm}b/a)J_n(k_\rho b)-\psi_n(\beta_{nm})J_n(k_\rho a)\end{aligned} \tag{14}$$

Orthogonal system

$$\boldsymbol{f}_{np}(\rho)=\begin{cases}\begin{bmatrix}\frac{n}{\alpha_{np}\rho/a}\phi(\alpha_{np}\rho/a)\\ \phi'(\alpha_{np}\rho/a)\end{bmatrix} & a<\rho<b\\ 0 & \rho>b,\rho<a\end{cases} \tag{15}$$

The Hankel transform of $\boldsymbol{f}_{np}$ is:

$$\boldsymbol{F}_{np}(k_\rho)=\begin{bmatrix}0\\ \frac{k_\rho a}{k_\rho^2-(\alpha_{np}/a)^2}Z_{np}(k_\rho)\end{bmatrix} \tag{16}$$

Where

$$\phi_n(\alpha_{np}\rho/a)=J_n(\alpha_{np}\rho/a)Y_n(\alpha_{np})-J_n(\alpha_{np})Y_n(\alpha_{np}\rho/a) \tag{17}$$

$$\phi_n(\alpha_{np}b/a)=\phi_n(\alpha_{np})=0 \tag{18}$$

$$Z_{np}(\rho)=\frac{b}{a}\phi_n'(\alpha_{np}b/a)J_n(k_\rho b)-\phi_n'(\alpha_{np})J_n(k_\rho a) \tag{19}$$

Vector Hankel transform of the current basis functions can be written as:

$$\boldsymbol{K}_n\ (k\rho)=\sum_{m=1}^{M}a_{nm}\boldsymbol{L}_{nm}\ (k\rho)+\sum_{q=1}^{Q}b_{nq}\boldsymbol{F}_{nq}\ (k\rho) \tag{20}$$

The expression of the spectral dyadic Green function of the stratified medium, in which the patch is embedded, is shown to be given by : (Losada, Boix, & Horno, 1999) (Benmeddour, Benabdelaziz, Bouttout, & Aouabdia, 2004) (Benmeddour, Dumond, Benabdelaziz, & Bouttout, 2011).

$$\boldsymbol{E}(k_\rho)=\boldsymbol{G}(k_\rho)\times\boldsymbol{\kappa}(k_\rho) \tag{21}$$

$$\boldsymbol{e}_n(\rho)=\int_0^\infty dk_\rho k_\rho\bar{\boldsymbol{H}}_n\left(k_\rho\rho\right).\left(\bar{\boldsymbol{G}}(k_\rho)-\bar{\boldsymbol{Z}}_s\right).\bar{\boldsymbol{K}}_n(k_\rho)=0\quad a<\rho<b \tag{22}$$

$$\boldsymbol{\kappa}_\rho=\int_0^\infty dk_\rho k_\rho\bar{\boldsymbol{H}}_n\left(k_\rho\rho\right).\bar{\boldsymbol{K}}_n(k_\rho)=0\qquad \rho>b,\ \rho<a \tag{23}$$

Where

The electric field integral equation which enforces the boundary condition must vanish on the patch surface, as discretized into a matrix form shown as:

(24)

$$\begin{bmatrix} \left(\bar{Z}'^{\psi\psi}\right)_{M\times M} & \left(\bar{Z}'^{\psi\varphi}\right)_{M\times P} \\ \left(\bar{Z}'^{\varphi\psi}\right)_{P\times M} & \left(\bar{Z}'^{\varphi\varphi}\right)_{P\times P} \end{bmatrix} \cdot \begin{bmatrix} \left(A'\right)_{M\times 1} \\ \left(B'\right)_{P\times 1} \end{bmatrix} = 0$$

Each element of the submatrices $\bar{Z}_{ij}^{CD}$ is given by:

$$\bar{Z}'^{CD}_{ij} = \int_0^\infty dk_\rho k_\rho C_{ni}^{+}(k_\rho)\cdot G(k_\rho)\cdot D_{nj}(k_\rho) \tag{25}$$

Where
$\boldsymbol{C}$ and **D** represent either $\boldsymbol{\varphi}$ or $\boldsymbol{\psi}$ for every value of the integer $\boldsymbol{n}$.

The system of linear equation has non-trivial solutions when the determinant of system equation (30) vanishes, that is:

$$\mathbf{det}\left([\bar{Z}'(f)]\right) = 0 \tag{26}$$

The equation (26) is the characteristic equation of the complex resonant frequencies of the microstrip antenna having stacked configuration as shown in figure 1.
The real parts of the complex resonant frequencies correspond to the resonant frequencies of the antenna, whereas, the imaginary parts are due to radiation loss of the antenna. Once the resonant frequencies are obtained, we can determinate the half power bandwidth.

$$BW = 2f_i / f_r \tag{27}$$

With f_i is the imaginary part of the resonant frequency, and is f_r the real part of the resonant frequency.

Numerical results and discussions

Validation of results

In order to confirm the computation accuracy of the approach described in the previous section, our numerical results are compared with those obtained from other works Table 1 shows the calculated resonant frequencies for the modes of Annular-ring Microstrip Single Layer Antenna (TM^{11},TM^{21}, andTM^{31}). These results are compared with theoretical and experimental data, which have been suggested in (Richard, Bhasin, & Claspy, 1993) (Lee, Yho, & Dahel, 1984) (Lee & Dahele, The two-layered annular ring microstrip antenna, 1986).
The annular patch is printed on a substrate of thickness $h_1 = 1.59mm$, and $b = 2a$.
Note that the agreement between our computed results and experimental and the theoretical results is very good.

Table 1. Comparison of measured and theoretical resonant frequencies for different modes TM^{11}, TM^{21}, TM^{31}, $\varepsilon_{r1} = 2{,}32$, $b = 2a$, $h_1 = 1.59mm$ $h_2 = 0mm$

Modes	ε_{r1}	a [Cm]	Measured frequencies f_r[GHz]	Calculated frequencies f_r[GHz]		
			(Richard, Bhasin, & Claspy, 1993)	(Lee, Yho, & Dahel, 1984)	(Lee & Dahele, The two-layered annular ring microstrip antenna, 1986)	This paper
TM^{11}	2.32	2.5	0.877	0.878	0.875	0.876
TM^{21}	2.32	2.5	1.722	1.723	1.732	1.732
TM^{31}	2.32	2.5	2.517	2.515	2.556	2.525
TM^{11}	2.32	3.5	0.626	0.623	0.621	0.622

Table 2. Comparison and calculated resonant wave number times the inner radius of the ring (k_r)

h_1/a	Mode TM^{11}					
	Results of (Gomez-Tagle & Christodoulou, 1997)			Our results		
	Re $(k_r a)$	Im $(k_r a)$	BP%	Re $(k_r a)$	Im $(k_r a)$	BP%
0.005	0.67	$1.6.10^{-4}$	0.048	0.676	$1.6.10^{-4}$	0.047
0.01	0.68	$1.7.10^{-4}$	0.05	0.682	$1.8.10^{-4}$	0.053
0.05	0.70	$5.4.10^{-4}$	0.15	0.695	$5.5.10^{-4}$	0.151
0.1	0.71	0.0012	0.34	0.705	0.0012	0.345

As a validation of the different results, in table 2, we have compared the results obtained with this theory and previously published data (Gomez-Tagle & Christodoulou, 1997). We have calculated the resonant wave number (k_r) times the inner radius a of the ring $k_r a$ ($(k_r\, a = 2\pi f_r \sqrt{\varepsilon_x \varepsilon_0 \mu_0})$, as functions of different sizes of the ratio of the substrate thickness h_1 normalized by the inner radius a (for the modes TM^{11}). The annular antenna printed on a substrate of permittivity $\varepsilon_{1x} = \varepsilon_{1z} = 2.65$, for the inner radius $a = 0.71cm$, thickness $h_2 = 0$ and the outer radius $b = 2a$ and, for various thickness h_1 .
Again, the comparisons show a good agreement between our results and those of literature.

Effet of Isotripic Superstrate

In this sub section, a rigorous analysis of the annular-ring printed patch is obtained using the vector Henkek transform and Galerkin's method. Figure 3 depicts the variation of the resonant characteristics for annular-ring printed antenna as function of thicknesses h_2 and permittivity ε_{r2} of superstrate.

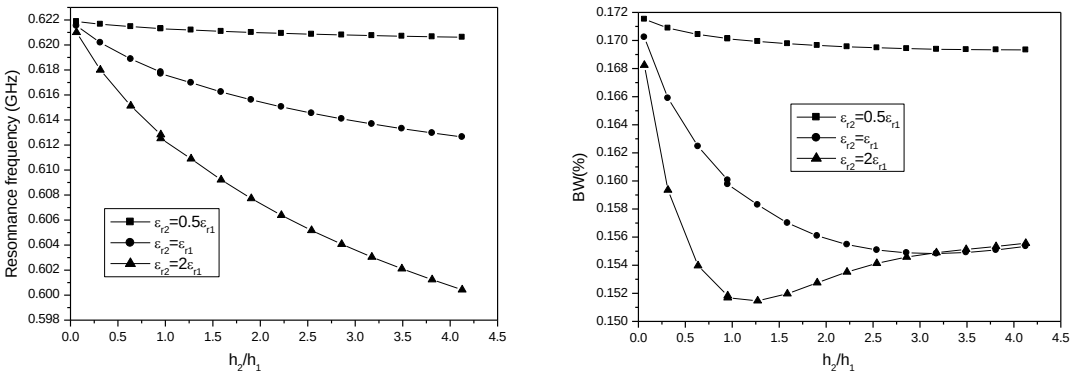

(a) (b)

Figure. 2. Resonance frequency and half-power bandwidth of the annular-ring printed antenna with different thicknesses of superstrate layer against permittivity of superstrate layer;
(a) Resonance Frequency, (b) Half-power bandwidth

Results show that in addition to its protective action, the presence of a dielectric cover has two major interests in the field of antennas: (1) it decreases the resonant frequency which allows a reduction in the patch size for the same target frequency and (2) it increases the half-power bandwidth which improves the narrow-band characteristics of printed antenna. It can be observed both in Fig. 2a. and 2b that these effects are more pronounced for thicker superstrate and for increasing ratio of $\varepsilon_{r2}/\varepsilon_{r1}$. As it is well-known in printed antenna design, a low value of substrate permittivity ε_{r1} is generally preferred because it increases the fringing field at the patch periphery and then the radiated power. Thus the use of high permittivity superstrate ε_{r2} leading to high ratio $\varepsilon_{r2}/\varepsilon_{r1}$ is possible and could give significant improvements in condition of sufficient thickness. Indeed, from Fig. 2b, we can note that for ratios h_2/h_1 less than 3.1, the bandwidth is degraded and this especially as the permittivity ε_{r2} of the superstrate is high.

Conclusion

This work presents the resonant characteristics of superstrate loaded annular printed antenna. The analysis has been based on a full-wave model with London's equations and the Gorter-Casimir two-fluid model. It is shown that resonant frequency of the Annular-Ring printed Antenna is seriously affected from the anisotropy of superstrate layer. These results indicate that the effect of the superstrate layer on the resonant characteristics of

the Annular-Ring printed Antenna is stronger for higher superstrate thickness and permittivity. The accuracy of our results has been checked with different approaches and shows a very good agreement. The optimal operating frequency of the structure is shifted and wider bandwidth operation is achieved. These results must be taken into account in shielding applications in order to avoid unwanted characteristics and better protection of the structure.

References

Garg, R., Bhartia, P., Bahl, I., & Ittipiboon, A. (1995). *Microstrip Antenna Design Handbook.* Norwood: MA: Artech House.

BahI, I., & Bbartia, P. (1980). *Microstrip Antennas.* USA: Dedham, Mass. : Artech House.

Balanis, C. (1997). *Antenna Theory: Analysis & Design* (éd. 2). New York, USA: John Wiley & Sons, Inc.

Benmeddour, F., Benabdelaziz, F., Bouttout, F., & Aouabdia, N. (2004). Resonance characteristics of circular microstrip antennas using moment method and various current representations. *First International Symposium on Control, Communications and Signal Processing*, 339-342.

Benmeddour, F., Dumond, C., Benabdelaziz, F., & Bouttout, F. (2011). Improving the performances of a high Tc superconducting circular microstrip antenna with multilayered configuration and anisotropic dielectrics. *18*, pp. 169-183.

Bhartia, P., Rao, K., & Tomar, R. (1991). *Millimeter Wave Microstrip and Printed Circuit Antennas* . Boston, London: Artech House.

Biswas, M., & Guha, D. (2009). Input impedance and resonance characteristics of the superstrate –loaded triangular Microstrip patch. *IET Microw. Antennas propag, 3*, pp. 92- 98.

Bouttout, F., Benabdelaziz, F., Benghalia, A., Khedrouche, D., & Fortaki, T. (1999). Uniaxialy anisotropic substrate effects on resonance of rectangular microstrip patch antenna. *Electonics. Letters, 35*(4), pp. 255-256.

Chew, W., & Kong, J. (1980). Resonance of non-axial symme- tric modes in circular micro strip disk. *Mathematical. Physics, 21*(10), pp. 2590-2598.

Gomez-Tagle, J., & Christodoulou, C. (1997, November). Extended cavity model analysis of stacked microstrip ring antenna. *IEEE Trans. Antennas Propagat, 45*(11).

Gurel, C., & Yazgan, E. (2003). The effects of uniaxially anisotropic superstrate shielding on the resonant characteristics of circular microstrip patch. *IEEE International Symposium on Electromagnetic Compatibility, 2003. EMC '03.* Istanbul, Turkey.

James, P. S. Hall, J., Hall, P., & Wood, C. (1981). *Microstrip Antenna Theory and Design.* London, U.K: Peter Peregrinus.

Kumar, G., & Ray, K. (2003). *Broadband Microstrip Antennas, Artech House, Boston London ISBN 1- 58053-244-6,*. Boston London: Artech House.

Lee, K., Luc, K., & Dahele, J. (1988, November). Characteristics of the equilateral triangular patch antenna. *IEEE Transactions on antennas and propagation, 36*(11), pp. 1510- 1518.

Lee, K., & Dahele, J. (1986). The two-layered annular ring microstrip antenna. *Int. J. Electronpp*, pp. 207-217.

Lee, K., Yho, K., & Dahel, J. (1984, August). Circular-disk microstrip antenna with an air gap. *Antennas and Propagation, IEEE Transactions, AP. 32*(8).

Losada, V., Boix, R., & Horno, M. (1999, April). Resonant Modes of Circular Microstrip Patches in Multilayered Substrates. *IEEE Transactions on Microwave Theory and Techniques, 47*(4), pp. 488–498.

Nicolaos, G., Alexopoulos, G., & Jackson, D. (1984). Fundamental Superstrate Effets on Printed circuit Antenna Efficiency. *IEEE MTT-S DIGEST*.

POZAR, D. (1983, September). Considerations for Millimeter Wave Printed Antennas. *IEEE TRANSACTIONS ON ANTENNAS AND PROPAGATION, 31*(5), pp. 740-747.

Richard, M., Bhasin, K., & Claspy, P. (1993, July). Superconducting microstrip antennas: an experimental comparison of two feeding methods. *Antennas and Propagation, IEEE Transactions, 41*, pp. 967 – 974.

Sami, M. A., Chew, W., & Kong, J. A. (1982, July). Vector Hankel transform analysis of annular ring microstrip antenna. *IEEE Transactions on Antennas and Propagation, AP-30*(4).

Sung, Y., & Kim, Y.-S. (2005, may). An Improved Design of Microstrip Patch Antennas Using Photonic Bandgap Structure. *IEEE transactions on antennas and propagation, 53*(5).

Author Information

Fadila Benmeddour
Electronics Department, University of M'Sila,
Laboratoire de Génie Electrique (LGE), M'sila, Algeria
benmeddourfadila@yahoo.fr
Contact E-mail: *fadila.benmeddour@univ-msila.dz*

Elhadi Kenane
Electronics Department, University of M'Sila,
Laboratoire de Génie Electrique (LGE), M'sila, Algeria

Christophe Dumond
Institut Prisme, IUT de Chartres,
Université d'Orléans,
Chartres, France